

Efficient NIR-Light Emission from Solid-State Complexes of Boron Difluoride with 2'-Hydroxychalcone Derivatives

Anthony D'Aléo,^{*,[a]} David Gachet,^[a] Vasile Heresanu,^[a] Michel Giorgi,^[b] and Frédéric Fages^{*,[a]}

Dedicated to Dr. Hubert Le Bozec on the occasion of his 60th birthday

Abstract: This article describes a series of nine complexes of boron difluoride with 2'-hydroxychalcone derivatives. These dyes were synthesized very simply and exhibited intense NIR emission in the solid state. Complexation with boron was shown to impart very strong donor–acceptor character into the excited state of these dyes, which further shifted their emission towards the NIR region (up to 855 nm for dye **5b**, which contained the strongly donating triphenylamine group). Strikingly, these optical features were obtained for crystalline solids, which are characterized by high molecular order and

tight packing, two features that are conventionally believed to be detrimental to luminescence in organic crystals. Remarkably, the emission of light from the π -stacked molecules did not occur at the expense of the emission quantum yield. Indeed, in the case of pyrene-containing dye **4**, for example, a fluorescence quantum yield of about 15% with a fluorescence emission maximum at 755 nm were obtained in the

solid state. Moreover, dye **3a** and acetonaphthone-based compounds **1b**, **2b**, and **3b** showed no evidence of degradation as solutions in CH_2Cl_2 that contained EtOH. In particular, solutions of brightly fluorescent compound **3a** (brightness: $\epsilon \times \Phi_f = 45\,000 \text{ M}^{-1} \text{ cm}^{-1}$) could be stored for long periods without any detectable changes in its optical properties. All together, these new dyes possess a set of very interesting properties that make them promising solid-state NIR fluorophores for applications in materials science.

Keywords: boron • chalcones • chromophores • dyes/pigments • near-infrared emission

Introduction

Light-emissive solids are key materials in a range of technologies, including chemical sensing, bioimaging, information displays and processing, and telecommunications.^[1] Although a large number of fully organic fluorophores have been found to be efficient in the visible spectrum, those that emit deep-red- or near-infrared (NIR) light with significant efficiency in the condensed phase still remain much less common.^[2] The most-popular NIR-emissive organic dyes belong to the class of polymethines^[3] but also include oxazine and thiazine derivatives,^[3] rylene,^[4] squaraines,^[5] borondipyromethanes (BODIPYs),^[6] and low-band-gap π -conjugated oligomers.^[7] Despite numerous studies, only very few of these compounds have been reported to be effective

as solid emitters and values of their photoluminescence quantum yields in the condensed phase are very scarce and usually low.

Chalcones are a well-known class of dyes^[8] that have found numerous applications in linear- and nonlinear-optical materials.^[9–12] Naturally-occurring chalcone-based pigments have been proposed as an attractive source of “green” materials for bio-organic electronics and -photonics.^[13] Although the solution-state photophysics of chalcones is well-documented,^[11] that of boron complexes of 2'-hydroxy-substituted analogues has received little attention^[12] and nothing is known about their solid-state fluorescence. This class of molecules was investigated for potential applications as laser dyes^[14] or dopants in photorefractive polymeric materials.^[15] The main limitation in the use of chalcones as fluorophores is their weak fluorescence efficiency in solution because excited-state dynamics in liquids is governed by intramolecular torsional motions and by photoisomerization processes, which offer privileged funnels for the radiationless deactivation of the first singlet excited state. 4-Substituted chalcones with electron-donating groups belong to the class of donor-acceptor (D–A) push-pull molecules and, thus, exhibit strongly Stokes-shifted fluorescence emission that can reach the NIR region in solution.^[11] Recent reports have described the ability of dipolar dyes^[16] and π -stacked charge-transfer (CT) complexes^[17] to display efficient emis-

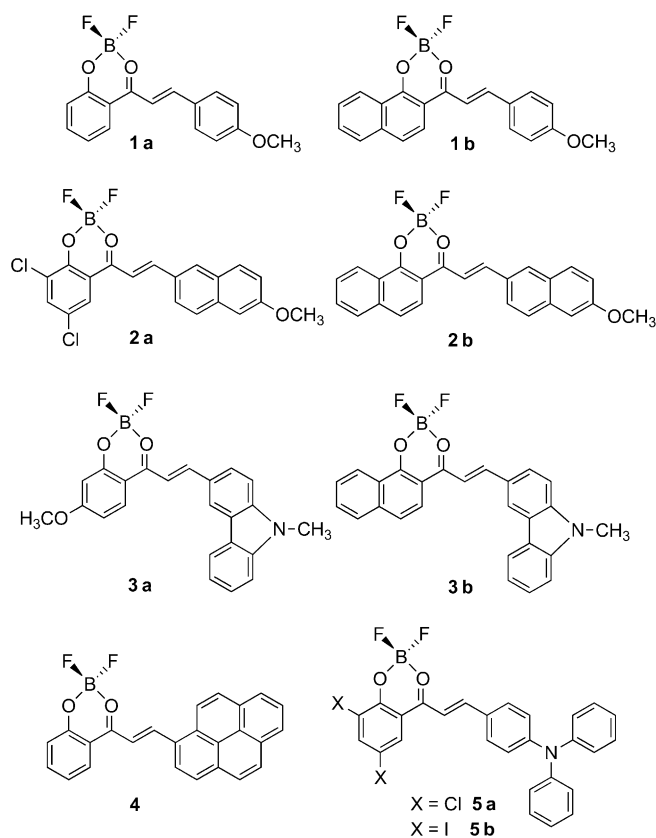
[a] Dr. A. D'Aléo, Dr. D. Gachet, Dr. V. Heresanu, Prof. F. Fages
Aix-Marseille Université, CNRS, CINaM UMR 7325
Campus de Luminy, Case 913, 13288 Marseille (France)
Fax: (+33) 491-829-301
E-mail: daleo@cinam.univ-mrs.fr
frederic.fages@univ-amu.fr

[b] Dr. M. Giorgi
Aix-Marseille Université, CNRS, Spectropole FR 1739
Campus Scientifique de Saint Jérôme, 13397 Marseille (France)

Supporting information for this article is available on the WWW under <http://dx.doi.org/10.1002/chem.201201812>.

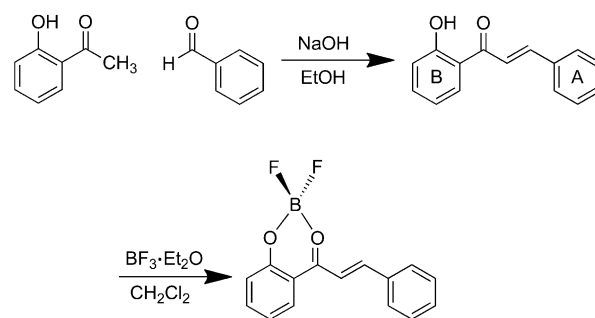
sion in the solid state; however, in these examples, emission occurred in the visible-light region. Thus, we decided to use boron-complexation with 2'-hydroxychalcones to further enhance the push-pull character of the arylpropenone skeleton, with the idea that the resulting decrease in the HOMO–LUMO gap could impart solid-state difluorodioxaborine chalcone dyes with NIR emission. During the course of our investigation on a broad series of boron-difluoride complexes of 2'-hydroxychalcones, we indeed observed that these compounds had a general propensity to deliver solid-state emission that ranged from visible- to NIR light depending on the molecular structure, which, to the best of our knowledge, has not been reported before.

Herein, we report on a selection of difluorodioxaborine chalcone derivatives (Scheme 1) that were chosen to illus-



Scheme 1. Structures of the boron-difluoride complexes of 2'-hydroxychalcones **1a/b**–**3a/b**, **4**, and **5a/b**.

trate some unprecedented NIR-emission properties. Compounds **2a/b**, **3a/b**, **4**, and **5a/b** are new, whilst the synthesis of compounds **1a** and **1b** has already been described in the literature but their photophysical properties were not reported.^[12] This series served to outline the influence of the nature of both the donor- and acceptor groups (A and B, respectively, Scheme 2) on solid-state optical properties. Compounds that contained carbazole (**3a/b**) and triphenylamine units (TPA, **5a/b**) were among the strongest push-pull structures that we have investigated so far. Methoxynaphthyl-



Scheme 2. Synthetic route to the 2'-hydroxychalcone skeleton and its boron-difluoride complex.

and pyrenyl aromatic groups, with their large dimensions and flat shape, represented attractive π -stacking units that have already been shown to be useful for the generation of optoelectronic materials.^[18] We show that replacing the acetophenone unit by acetonaphthone in part B (Scheme 2) not only affected the optical properties of the dyes but also provided a remarkable gain in stability in solution. Moreover, halogen atoms were also introduced onto the B ring because halogen–halogen interactions are known to have a significant influence on molecular arrangement in the crystal.^[19] Much to our surprise, compound **5b**, which contained two iodine atoms, was observed to be fluorescent in the solid state. Herein, we describe the spectroscopic properties of the difluorodioxaborine chalcones in solution and in the solid state. These results show that NIR fluorescence emission originates from electronically interacting fluorophores in tightly packed solid-state assemblies.

Results and Discussion

2'-Hydroxychalcone ligands **1a/b-H**, **2a/b-H**, **3a/b-H**, **4-H**, and **5a/b-H** were obtained very simply by using a Claisen–Schmidt reaction between various aldehydes and acetophenones/acetonaphthones in EtOH as the solvent and sodium hydroxide as a base (Scheme 2). Complexation to boron was performed quantitatively by reacting the ligands with a slight excess of boron trifluoride etherate in CH_2Cl_2 . Dyes **1a/b**, **2a/b**, **3a/b**, **4**, and **5a/b** were obtained as darkly colored solids and characterized by using ^1H -, ^{13}C - and ^{19}F NMR spectroscopy, MS, and elemental analysis.

None of the free ligands were fluorescent in solution or in the solid state, which was consistent with the propensity of 2'-hydroxychalcone derivatives to undergo facile excited-state intramolecular proton-transfer.^[20] BF_2 -complexation produced considerable red-shifts (>100 nm) of the maximum absorption wavelength in all of the compounds (Table 1; also see the Supporting Information, Figure S1) as a consequence of the enhanced dipolar character of the difluorodioxaborine-containing species. Intramolecular CT was evidenced by the positive solvatochromic shifts of both the absorption- and emission bands (see the Supporting Information, Figure S2). Concomitantly, BF_2 complexation

Table 1. Electronic absorption properties of the free 2'-hydroxychalcones and their complexes with BF₂ in CH₂Cl₂.

	Free ligands		BF ₂ complexes		$\Delta\lambda$ [cm ⁻¹] (nm)
	$\lambda_{\text{abs}}^{\text{max}}$ [nm]	ϵ [M ⁻¹ cm ⁻¹]	$\lambda_{\text{abs}}^{\text{max}}$ [nm]	ϵ [M ⁻¹ cm ⁻¹]	
1a	367	26300	455	41190	5270 (88)
1b	363	24680	486	37340	6970 (132)
2a	402	30230	510	45930	5270 (108)
2b	388	30895	501	49525	5815 (123)
3a	405	35456	504	56300	4850 (99)
3b	425	28690	538	47210	4940 (113)
4	432	28170	541	44190	4660 (109)
5a	464	33420	588	68910	4545 (122)
5b	465	32625	591	67320	4585 (126)

also led to a considerable increase in the oscillator strength of the lowest-energy transition band.

Whilst weak intramolecular CT emission in the difluorodioxaborine derivatives was recorded in general in CH₂Cl₂ solution, the carbazole-containing compounds (**3a/b**) exhibited very intense fluorescence with high quantum yield (Φ_f)

Table 2. Fluorescence-emission properties of BF₂ complexes of 2'-hydroxychalcones in CH₂Cl₂ at room temperature.

	$\lambda_{\text{em}}^{\text{max}}$ [nm]	$\Delta\lambda$ [cm ⁻¹]	Φ_f	τ [ns]
1a	556	3992	0.02	0.41
1b	609	4155	0.02	0.40
2a	608	2855	0.14	1.1
2b	602	3350	0.025	0.42
3a	584	2720	0.795	2.8
3b	595	1780	0.49	2.25
4	644	2956	0.29	1.6
5a	— ^[a]	— ^[a]	— ^[a]	— ^[a]
5b	— ^[a]	— ^[a]	— ^[a]	— ^[a]

[a] No emission (see text).

values (Table 2); in particular, compound **3a** ($\Phi_f = 79.5\%$ in CH₂Cl₂) possessed high optical brightness ($\epsilon \times \Phi_f = 45000 \text{ M}^{-1} \text{ cm}^{-1}$). The fluorescence-decay lifetimes were in the sub-nanosecond-to-nanosecond range (Table 2; also see the Supporting Information, Figure S3), which is in keeping with the known fast excited-state dynamics of chalcones in solution.^[11] The fluorescence emission in dyes **5a/b**, which contained the strong electron-donating TPA group, was totally quenched, irrespective of the nature of the solvent. The presence of the two heavy iodine atoms in compound **5b** was believed to favor intersystem crossing to the triplet excited state through an internal heavy-atom effect.

Because the hydrolytic cleavage of the BF₂ chelate is a possible pathway for the degradation of the compounds in solution, we spectrophotometrically investigated the stability of solutions of the dyes in CH₂Cl₂ that contained EtOH (0.5 vol %) as a competing Lewis base. Importantly, dye **3a** and acetophenone-based compounds **1b**, **2b**, and **3b** showed no evidence of degradation under these conditions. In the case of compounds **1a** and **1b**, Figure 1 shows the remarkable chemical stabilization effect of the acetophen-

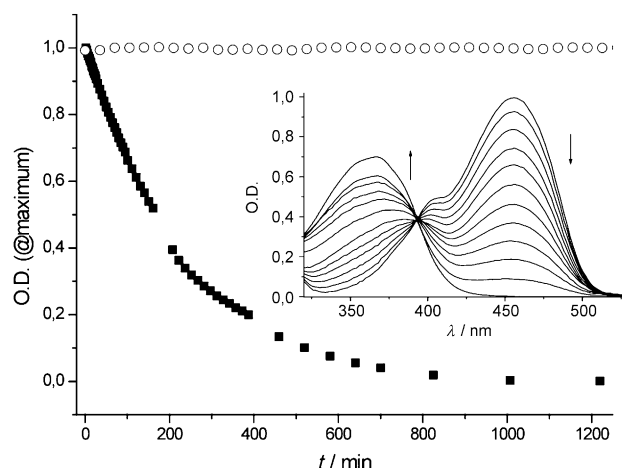


Figure 1. Kinetic stability in CH₂Cl₂ that contained 0.5 vol % EtOH at room temperature; the stability was monitored by measuring the absorbance decay at the maximum absorption wavelength of the BF₂ complexes for compounds **1a** (■) and **1b** (○). Inset: corresponding changes in the electronic absorption spectrum of compound **1b** as a function of time.

thone unit relative to its acetophenone counterpart. In particular, solutions of brightly fluorescent compound **3a** could be stored for long periods of time without any detectable changes in its optical properties. However, the remaining compounds were subject to solvolysis under the same conditions. The kinetics of decomplexation were followed by UV/Vis spectroscopy of the boron complexes at regular time intervals. Half-life values and kinetic rates were obtained by plotting the decay of the absorbance value at the maximum absorption wavelength versus time (Figure 1; also see the Supporting Information, Figure S4). The pseudo-first-order rate constant values (k_{obs}) for dyes **1a**, **2a**, **4**, and **5a/b** were in the range $5 \times 10^{-5} - 5 \times 10^{-4} \text{ s}^{-1}$ (see the Supporting Information, Table S1) and strongly increased with larger amounts of EtOH. Thus, manipulating solutions of this series of compounds necessitated the use of carefully dried solvents, whereas, in the case of inert dyes **1b**, **2b**, and **3a/b**, such drastic conditions were useless. We could even quickly dilute their solutions in THF (0.15 mL, 0.1 mM) with water (2.85 mL) at room temperature without observing any degradation. Under these conditions, precipitation was much faster than hydrolysis and stable suspensions of the aggregated dyes could be obtained. The generation of nanosized organic particles with NIR emission is a topical subject of investigation^[6f] and the BF₂-chalcone dyes might represent attractive candidates to this end. At this stage of the work, we had not as yet attempted to optimize the synthesis of the particles and control their size-distribution; hence, relatively large particles were generated (about 900 nm for compound **1b**; see the Supporting Information, Figure S5). In fact, they were particularly useful for spectroscopic investigation (see below). Moreover, it is important to note that all BF₂-chalcones investigated herein displayed indefinite air- and moisture-stability in the solid state and were stored under ambient conditions.

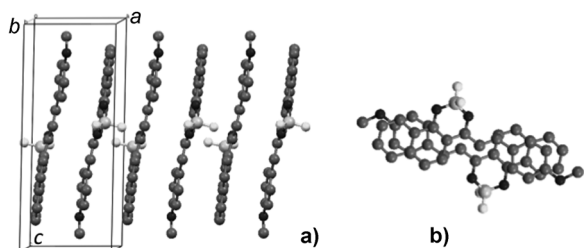


Figure 2. Molecular packing of compound **1b**, as determined by single-crystal X-ray diffraction: a) view along the *ac* plane, which shows the packing of the BF_2 complexes of chalcones; b) view of the π -stacks along the *a* axis. Hydrogen atoms are omitted for clarity.

We obtained crystals of dye **1b** that were suitable for single-crystal X-ray structure analysis (Figure 2; also see the Supporting Information, Figure S6 and Table S2).^[21] Comparison of the crystal structure of compound **1b** with that previously reported^[12a] for compound **1a** shows that both dyes display an almost-coplanar π -conjugated system. As has been seen in the crystals of dipolar chromophores,^[22] antiparallel molecular packing leads to discrete 1D π -stacks along the crystallographic *a* axis for both compounds **1a** and **1b**. We note a face-to-face superimposition of the π -conjugated system of dye **1b** with an almost equal interplanar distance (3.52 Å) along the stacks, whilst molecules of compound **1a** feature a kind of pairwise association. Within the tighter dimer unit (3.48 Å), molecules of compound **1a** are longitudinally displaced with respect to each other, thereby reducing the π contact area. In contrast, adjacent molecules of neighboring dimers (3.54 Å) experience full π -overlap, as in the case of **1b**. The molecular planes in the π -stacks are canted relative to the stacking *a* axis by 26.8° and 17° in compounds **1a** and **1b**, respectively. Unlike in compound **1a**, molecules of compound **1b** form parallel chains, in which the head-to-tail dipoles are aligned along the *c* axis with a distance of 4.56 Å between the naphthalene-end of one molecule and the anisole-end of the following molecule (see the Supporting Information, Figure S7). These chains are connected together through F–H contacts (2.66 Å) and form sheets parallel to the (100) planes. As a result, the structure is lamellar; in turn, the sheets that are packed antiparallel along the *a* axis generate the aforementioned π -stacks. The powder-diffraction patterns, as calculated from the single-crystal structures of compounds **1a/b**, were in perfect agreement with the experimental values (see the Supporting Information, Figures S8 and S9). Except for compound **5a**, which was amorphous, the remaining compounds gave high-quality crystalline samples (see the Supporting Information, Figure S10).

The solid-state electronic absorption properties of thin films that were drop-cast from solutions in CH_2Cl_2 were investigated in transmission mode (Figure 3a; also see the Supporting Information, Figure S11). According to the trends in their optical properties, BF_2 -chalcones **1–4** can be classified into three types: First, the absorption spectrum of compound **1a** was hypsochromically shifted relative to the

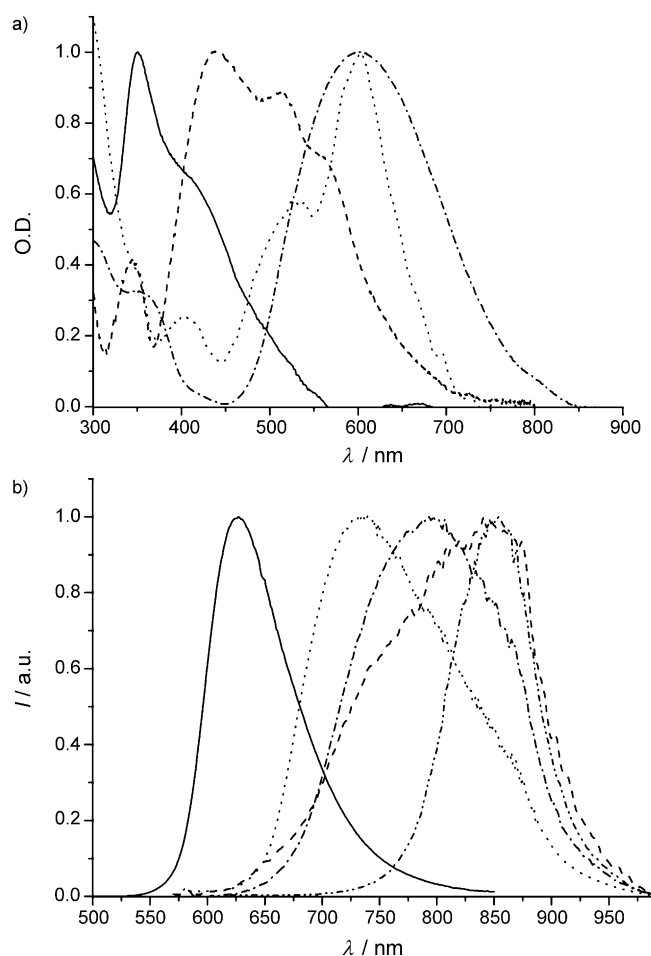


Figure 3. Optical properties of the thin solid-films: a) normalized absorption spectra of compounds **1a** (—), **1b** (---), **2a** (.....), and **5a** (-.-.); b) normalized emission spectra of compounds **1a** (—), **1b** (---), **2b** (.....), **3b** (-.-.), and **5b** (-.-.-).

solution, thereby featuring a H-like transition band,^[23] which correlated with solid-state chromophore-organization. Second, compounds **1b**, **2b**, **3a/b**, and **4** displayed complex absorption spectra that were characteristic of excitons that originated from chromophores with parallel- and antiparallel transition dipoles. This situation is typically the one that occurs in the crystal of compound **1b**, in which π -stacks and dipole chains provide the adequate molecular arrangements for Davydov splitting into high- and low-energy components, respectively.^[24] Finally, the absorption profile of dye **2a** contained a strongly bathochromically shifted band with a smaller Stokes shift (2640 cm^{-1}) relative to the other compounds. This value was even smaller than that recorded for a solution in CH_2Cl_2 (2855 cm^{-1}). These peculiar features suggest the formation of J-like assemblies^[23,25] that are presumably directed by the participation of the chlorine atoms in lattice-stabilization.

All of these compounds were found to be emissive in the solid state (Table 3, Figure S11). The highly crystalline powders exhibited emission profiles that were identical to those of the thin films and colloidal particles. In the case of com-

Table 3. Spectroscopic properties of boron-difluoride complexes of 2'-hydroxychalcones **1a/b**–**3a/b**, **4**, and **5a/b** in the solid state.

	$\lambda_{\text{abs}}^{\text{max}}$ [nm]	$\lambda_{\text{em}}^{\text{max}}$ [nm]	$\Delta\lambda$ [cm^{-1}]	Φ_{f} [%]
1a	351, 418(s) ^[a]	627	7975	21.0
1b	438, 515, 562	845	5959	0.5
2a	534, 603	722	2733	19.5
2b	464, 521, 570(s) ^[a]	736	3957	2.5
3a	424, 456, 536(s) ^[a]	717	4710	8.0
3b	487, 545, 587	796	4473	1.5
4	565, 626(s) ^[a]	755	2729	15.5
5a	602	850	4847	0.5
5b	620	855	4433	0.1

[a] Shoulder.

pound **1b**, excitation at the red edge or at the maximum of the absorption band of a single crystal, a powder sample, and a thin film all resulted in the same fluorescence spectrum. These spectra displayed a broad emission band with a maximum beyond 700 nm, except for compound **1a** (627 nm; Figure 3b). The red-shifts were about 100–155 nm (**1a**: 71 nm) relative to the solution. Compared to organic solids that emit in the deep-red/NIR region, the four dyes **1b**, **2b**, and **3a/b** (with similar ground-state spectroscopic features) displayed high Φ_{f} values that decreased with decreasing energy-gap. These compounds also displayed large Stokes shifts (4000–6000 cm^{-1}), larger than their values in solution, especially for dyes **3a/b**, which contained the strongly electron-donating carbazolyl group. Whilst the solid-state Φ_{f} values for compounds **1b**, **2b**, **3a/b**, and **4** were somewhat lower than their values in solution, compounds **1a** and **2a** featured a marked opposite effect with higher Φ_{f} (about 20%) in the solid state relative to their values in solution (see the Supporting Information, Figure S12). Such a value for solids that emit in the visible range is not uncommon but it is noteworthy that it was obtained herein for compound **1a**, which adopted the H-like aggregation mode. Moreover, dyes **2a** and **4** displayed the highest Φ_{f} values (19.5% at 722 nm and 15.5% at 755 nm, respectively) reported to date for a solid-state organic dye with fluorescence emission at a wavelength beyond 700 nm. Recently values of 6% at 743 nm^[6f] and 30% at 702 nm^[7b] were reported and represented to date the highest values found in literature.

D–A dyes are known to experience dipole-induced molecular interactions in the condensed phase. To enhance the radiative exciton relaxation in such systems, efforts have been directed towards preventing the close packing in the solid state by using, for example, bulky groups or spiro kinks.^[1] The impeding of dipole–dipole interactions was also found to be effective in symmetrical molecular frameworks that were built with the D–A–D (or A–D–A) electronic structure.^[7] In that respect, BF_2 -chalcones behaved very differently in the sense that their optical properties were recorded for crystalline solids that were characterized by molecular order and tight packing, two features that are conventionally thought to be detrimental to luminescence in organic crystals. We surmise that this situation could explain the lower-

ing of the emitting energy level, thereby leading to emission wavelengths in the deep-red- and NIR regions. Remarkably, the emission of light from π -stacked molecules did not operate at the expense of the emission quantum yield in the case of, for example, compounds **2a** or **4**. This observation is consistent with several theoretical- and experimental studies that have provided evidence for efficient fluorescence emission in tightly-packed π -conjugated systems^[26] and especially in solid-state dipolar dyes.^[16] Interestingly, harnessing electronic interactions between aromatic units within multichromophoric assemblies has served to produce unique photophysical properties.^[17,27] To account for the remarkable emission properties of the BF_2 complexes of the 2'-hydroxychalcones, other factors can also be invoked. Chromophore-planarization, as seen in the crystal structures of compounds **1a/b** and presumably also in the other compounds, can largely contribute to enhance the exciton radiative relaxation and to ensure red-shifted absorption and emission in the solid state with respect to the solution. Such a shift was even larger than that in polar acetonitrile. As was rationalized for dyes that are subject to aggregation-induced emission phenomena,^[1b] the favored solid-state fluorescence may also stem from the restriction of photoisomerization and intramolecular torsional motions, which are actually two very efficient processes for chalcones in solution.^[11] Moreover, owing to the dipolar character of the BF_2 -chalcones, large Stokes shifts were obtained, which may contribute to the decreased self-quenching in the condensed phase because of reduced spectroscopic overlap.^[28] The solid-state-emission characteristics of these molecules are clearly connected with their tight crystalline packing arrangement.^[29] In particular, the manner in which the fluorophores are assembled has been shown to be critical in the generation of solid-state CT complexes with enhanced emission intensity.^[17] Understanding the fate of excited states and, in particular, unraveling the mutual contribution of intramolecular and interchromophoric CT excitons in these materials will require in-depth experimental investigation and theoretical analysis.^[7a,30]

TPA-containing dyes **5a/b** followed a different behavior. Although only compound **5a** was obtained as an amorphous solid, both compounds were found to be filmogenic when drop-cast from CH_2Cl_2 , thereby forming glass-like, dark-colored deposits with nice optical quality. Their absorption spectra displayed a broad transition band that extended from 400 to 800 nm (Figure 2a; also see the Supporting Information, Figure S11). Outstandingly, compounds **5a** and **5b** exhibited solid-state emission at 850 and 855 nm, respectively (Figure 2b; also see the Supporting Information, Figure S11). The Φ_{f} values were low, especially when comparing compound **5a** (0.35%) with compound **2a**, but one has to note that both compounds **5a** and **5b** were not emissive in solution. In the case of compound **5b**, the emission-decay lifetime did not exceed 4 ns in the solid state, which was evidence for fluorescence as a radiative deactivation process. The emission spectrum of a frozen solution of compound **5b** at 77 K was located at higher energy relative to that of the thin film (see the Supporting Information, Figure S13) and a

photoluminescence lifetime value in the range of several microseconds could be obtained, thus indicating the participation of the triplet manifold at low temperature.

Conclusion

In conclusion, we have prepared a series of BF₂ complexes of 2'-hydroxychalcone derivatives that display high stability in solution and in the solid-state, large Φ_f values in solution, and intense NIR emission in closely packed solids. These dyes were obtained in a straightforward manner according to expeditious preparation- and facile purification procedures. We are currently working towards the synthesis of analogues with increased emission efficiency at wavelengths well-beyond the 800 nm threshold. Moreover, materials that are based on closely-packed dipolar dyes have recently been shown to benefit from high charge-mobility.^[31] Future work will also involve evaluating the semiconducting properties of BF₂-containing chalcones and exploiting their NIR emission and panchromatic absorption in displays and in solar-energy technologies.

Experimental Section

General procedures: All solvents for the syntheses were of analytic grade; spectroscopic measurements were carried out with spectroscopic-grade solvents. NMR spectra (¹H, ¹³C, and ¹⁹F) were recorded at RT on a BRUKER AC 250 that operated at 250, 62.5, and 235 MHz for ¹H-, ¹³C-, and ¹⁹F nuclei, respectively. Data are listed in parts per million (ppm) and are reported relative to tetramethylsilane (¹H and ¹³C); residual solvent peaks of the deuterated solvents were used as an internal standard. MS and elemental analysis were performed at the Spectropole de Marseille (<http://www.spectropole.fr>).

General synthesis: In a 100 mL round-bottomed flask, derivatives of 2'-hydroxyacetophenone or 1'-hydroxyacetophenone (1 molequiv) and the appropriate aldehyde (1 molequiv) were dissolved in EtOH. Subsequently, a solution of sodium hydroxide (2.5 molequiv) in water (1 mL) was added to the solution and the mixture was stirred for 16 h at 60°C. After cooling, the solution was acidified to pH 1 and the precipitate was filtered through glass filter funnel. The solid was the recrystallized twice from CH₂Cl₂/EtOH 1:1 to yield the pure 2'-hydroxychalcone ligands **1a/b-H**, **2a/b-H**, **3a/b-H**, **4**, and **5a/b-H**. In a 50 mL round-bottomed flask, the 2'-hydroxychalcone derivatives (1 molequiv) was dissolved in CH₂Cl₂. Boron trifluoride etherate (1.2 molequiv) was added and the solution was heated at reflux for 2 h. The solution was concentrated, cooled to RT, and the precipitate was filtered off, cleaned with Et₂O, and dried in air to yield the pure dyes **1a/b**, **2a/b**, **3a/b**, **4**, and **5a/b**.

1a-H: Yield: 21%; ¹H NMR (250 MHz, CDCl₃): δ = 12.98 (s, 1H), 7.96 (m, 1H), 7.94 (d, ³J(H,H) = 15.3 Hz, 1H), 7.66 (d, ³J(H,H) = 8.8 Hz, 1H), 7.57 (d, ³J(H,H) = 15.3 Hz, 1H), 7.52 (m, 1H), 7.01 (m, 2H), 6.95 (d, ³J(H,H) = 8.8 Hz, 1H), 3.90 ppm (s, 3H); ¹³C NMR (62.5 MHz, CDCl₃): δ = 193.69, 163.56, 162.04, 145.37, 136.16, 130.57, 129.54, 127.35, 120.13, 118.76, 118.60, 117.60, 114.53, 55.47 ppm.

1a: ¹H NMR (250 MHz, CDCl₃): δ = 8.53 (d, ³J(H,H) = 15.3 Hz, 1H), 7.96 (dd, ³J(H,H) = 8.0 Hz, ³J(H,H) = 1.0 Hz, 1H), 7.80 (d, ³J(H,H) = 9.0 Hz, 2H), 7.78 (m, 1H), 7.52 (d, ³J(H,H) = 15.0 Hz, 1H), 7.19 (dd, ³J(H,H) = 8.8 Hz, ⁴J(H,H) = 0.8 Hz, 1H), 7.07 (m, 1H), 7.05 ppm (d, ³J(H,H) = 8.8 Hz, 2H); ¹⁹F NMR (235 MHz, CDCl₃): δ = -142.22 (¹⁰B-F, 0.2), -142.28 ppm (¹¹B-F, 0.8).

1b-H: Yield: 28%; ¹H NMR (250 MHz, CDCl₃): δ = 14.78 (s, 1H), 8.34 (td, ³J(H,H) = 8.3 Hz, ⁴J(H,H) = 0.8 Hz, 1H), 7.81 (d, ³J(H,H) = 15.3 Hz, 1H), 7.69 (d, ³J(H,H) = 9.0 Hz, 1H), 7.61 (d, ³J(H,H) = 7.5 Hz, 1H), 7.48 (m, 3H), 7.42 (m, 1H), 7.40 (d, ³J(H,H) = 15.0 Hz, 1H), 7.14 (d, ³J(H,H) = 8.5 Hz, 1H), 7.80 (d, ³J(H,H) = 8.5 Hz, 1H), 3.71 ppm (s, 3H); ¹³C NMR (62.5 MHz, CDCl₃): δ = 193.19, 164.26, 161.98, 144.94, 137.31, 130.52, 130.02, 127.55, 127.37, 125.83, 125.57, 124.47, 123.95, 118.07, 117.98, 114.52, 113.54, 55.42 ppm.

1b: ¹H NMR (250 MHz, CDCl₃): δ = 8.68 (td, ³J(H,H) = 8.3 Hz, ⁴J(H,H) = 1.0 Hz, 1H), 8.48 (d, ³J(H,H) = 15.0 Hz, 1H), 7.78 (m, 4H), 7.69 (d, ³J(H,H) = 9.3 Hz, 1H), 7.62 (m, 1H), 7.54 (d, ³J(H,H) = 15.0 Hz, 1H), 7.35 (td, ³J(H,H) = 9.3 Hz, ⁴J(H,H) = 0.8 Hz, 1H), 7.05 (d, ³J(H,H) = 8.8 Hz, 2H), 3.95 ppm (s, 3H); ¹⁹F NMR (235 MHz, CDCl₃): δ = -140.88 (¹⁰B-F, 0.2), 140.94 ppm (¹¹B-F, 0.8).

2a-H: Yield: 58%; ¹H NMR (250 MHz, CDCl₃): δ = 13.49 (s, 1H), 8.13 (d, ³J(H,H) = 15.3 Hz, 1H), 8.03 (s, 1H); 7.86 (d, ⁴J(H,H) = 2.7 Hz, 1H), 7.79 (m, 3H), 7.60 (d, ³J(H,H) = 15.3 Hz, 1H), 7.59 (d, ⁴J(H,H) = 2.5 Hz, 1H), 7.19 (m, 2H), 3.95 ppm (s, 3H); MS (ESI positive mode): *m/z*: 373.1 [M+H]⁺; MS (ESI negative mode): *m/z*: 371.0 [M-H]⁻; elemental analysis calcd (%) for C₂₀H₁₄Cl₂O₃·1/6 CH₂Cl₂: C 62.53, H 3.73; found: C 62.65, H 3.72.

2a: Because of low solubility, NMR spectra could not be recorded. MS (ESI positive mode): *m/z*: 443.0 [M+Na]⁺, 459.0 [M+K]⁺; elemental analysis calcd (%) for C₂₀H₁₃BF₂Cl₂O₃·1/4 CH₂Cl₂: C 54.99, H 3.08; found: C 54.78, H 3.08.

2b-H: Yield: 69%; ¹H NMR (250 MHz, CDCl₃): δ = 14.96 (s, 1H), 8.51 (d, ³J(H,H) = 8.5 Hz, 1H), 8.11 (d, ³J(H,H) = 15.3 Hz, 1H), 8.00 (s, 1H), 7.88 (d, ³J(H,H) = 9.0 Hz, 1H), 7.78 (m, 5H), 7.64 (t, ³J(H,H) = 7.0 Hz, 1H), 7.54 (t, ³J(H,H) = 7.8 Hz, 1H), 7.31 (d, ³J(H,H) = 9.0 Hz, 1H), 7.18 (m, 2H), 3.94 ppm (s, 3H); ¹³C NMR (62.5 MHz, CDCl₃): δ = 193.16, 164.37, 159.14, 145.44, 137.35, 136.08, 130.88, 130.33, 130.17, 130.09, 128.76, 127.60, 127.38, 125.87, 125.56, 124.50, 124.48, 123.96, 119.58, 119.39, 118.13, 113.56, 106.10, 55.40 ppm; MS (ESI positive mode): *m/z*: 355.1 [M+H]⁺; MS (ESI negative mode): *m/z*: 353.1 [M-H]⁻; elemental analysis calcd (%) for C₂₄H₁₈O₃·1/4 CH₂Cl₂: C 77.54, H 4.96; found: C 77.72, H 5.03.

2b: Because of low solubility, NMR spectra could not be recorded. MS (ESI positive mode): *m/z*: 425.1 [M+Na]⁺, 441.1 [M+K]⁺; elemental analysis calcd (%) for C₂₄H₁₇BF₂O₃·1/2 CH₂Cl₂: C 66.18, H 4.08; found: C 65.72, H 4.16.

3a-H: Yield: 54%; ¹H NMR (250 MHz, CDCl₃): δ = 13.69 (s, 1H), 8.35 (d, ⁴J(H,H) = 1.3 Hz, 1H), 8.13 (d, ³J(H,H) = 8.5 Hz, 1H), 8.11 (d, ³J(H,H) = 15.5 Hz, 1H), 7.89 (d, ³J(H,H) = 9.3 Hz, 1H), 7.78 (dd, ³J(H,H) = 8.8 Hz, ⁴J(H,H) = 1.5 Hz, 1H), 7.60 (d, ³J(H,H) = 15.3 Hz, 1H), 7.52 (dd, ³J(H,H) = 8.3 Hz, ⁴J(H,H) = 1.3 Hz, 1H), 7.39 (m, 2H), 7.30 (dd, ³J(H,H) = 7.8 Hz, ⁴J(H,H) = 1.8 Hz, 1H), 6.50 (m, 2H), 3.86 (s, 3H), 3.85 ppm (s, 3H); ¹³C NMR (62.5 MHz, CDCl₃): δ = 191.86, 166.59, 165.89, 146.02, 142.53, 141.53, 131.11, 126.54, 126.42, 125.88, 123.35, 122.66, 121.58, 120.50, 119.83, 116.97, 114.29, 108.90, 107.48, 101.06, 55.53, 29.24 ppm; MS (ESI positive mode): *m/z*: 358.1 [M+H]⁺; MS (ESI, negative mode): *m/z*: 356.1 [M-H]⁻; elemental analysis calcd (%) for C₂₂H₁₉NO₃·1/5 CH₃CH₂OH: C 76.66, H 5.55, N 3.82; found: C 76.79, H 5.47, N 3.80.

3a: ¹H NMR (250 MHz, CDCl₃): δ = 8.57 (d, ³J(H,H) = 14.8 Hz, 1H), 8.43 (d, ⁴J(H,H) = 1.3 Hz, 1H), 8.10 (d, ³J(H,H) = 8.3 Hz, 1H), 7.82 (m, 2H), 7.43 (m, 4H), 7.29 (d, ³J(H,H) = 7.5 Hz, 1H), 6.50 (m, 2H), 3.77 (s, 3H), 3.75 ppm (s, 3H); ¹⁹F NMR (235 MHz, CDCl₃): δ = -142.98 (¹⁰B-F, 0.2F), -143.04 ppm (¹¹B-F, 0.8F); MS (ESI positive mode): *m/z*: 428.1 [M+Na]⁺, 444.1 [M+K]⁺; elemental analysis calcd (%) for C₂₂H₁₈BF₂NO₃·1/8 CH₂Cl₂: C 66.80, H 4.42, N 3.37; found: C 66.81, H 4.50, N 3.58.

3b-H: Yield: 63%; ¹H NMR (250 MHz, CDCl₃): δ = 15.14 (s, 1H), 8.51 (d, ³J(H,H) = 8.0 Hz, 1H), 8.43 (s, 1H), 8.24 (d, ³J(H,H) = 15.3 Hz, 1H), 8.17 (d, ³J(H,H) = 8.0 Hz, 1H), 7.95 (d, ³J(H,H) = 8.8 Hz, 1H), 7.81 (m, 3H), 7.64 (t, ³J(H,H) = 8.5 Hz, 1H), 7.54 (m, 2H), 7.44 (d, ³J(H,H) = 8.3 Hz, 2H), 7.32 (m, 2H), 3.89 ppm (s, 3H); ¹³C NMR (62.5 MHz, CDCl₃): δ = 193.17, 164.23, 146.78, 142.69, 141.58, 137.27, 129.93, 127.39,

126.74, 126.51, 125.92, 125.78, 125.63, 124.47, 124.09, 123.44, 122.71, 121.83, 120.57, 119.93, 177.99, 117.19, 113.66, 108.99, 108.94, 29.31 ppm; MS (ESI positive mode): m/z : 378.0 $[M+H]^+$; MS (ESI negative mode): m/z : 376.1 $[M-H]^-$; elemental analysis calcd (%) for $C_{26}H_{19}NO_2 \cdot 1/4 CH_2Cl_2$: C 79.08, H 4.93, N 3.51; found: C 79.39, H 4.87, N 3.55.

3b: Because of low solubility, NMR spectra could not be recorded. MS (ESI positive mode): m/z : 447.9 $[M+Na]^+$, 463.9 $[M+K]^+$; elemental analysis calcd (%) for $C_{26}H_{18}BF_2NO_2 \cdot 1/3 (C_2H_5)_2O$: C 72.96, H 4.78, N 3.11; C 72.73, H 4.45, N 3.26.

4-H: Yield: 64%; 1H NMR (250 MHz, $CDCl_3$): δ = 13.02 (s, 1H), 9.11 (d, $^3J(H,H)$ = 15.3 Hz, 1H), 8.59 (d, $^3J(H,H)$ = 9.3 Hz, 2H), 8.44 (d, $^3J(H,H)$ = 8.3 Hz, 1H), 8.12 (m, 8H), 7.94 (d, $^3J(H,H)$ = 15.3 Hz, 1H), 7.56 (m, 1H), 7.05 ppm (m, 2H); ^{13}C NMR (62.5 MHz, $CDCl_3$): δ = 193.40, 163.75, 142.04, 136.40, 133.26, 131.29, 130.69, 130.58, 129.71, 129.01, 128.95, 128.32, 127.32, 126.41, 126.26, 126.10, 125.06, 124.99, 124.56, 124.27, 122.46, 121.86, 120.19, 118.91, 118.70 ppm; MS (ESI positive mode): m/z : 349.0 $[M+H]^+$; MS (ESI negative mode): m/z : 347.1 $[M-H]^-$; elemental analysis calcd (%) for $C_{25}H_{16}O_2$: C 86.19, H 4.63; found: C 86.17, H 4.54.

4: Because of low solubility, NMR spectra could not be recorded. MS (ESI positive mode): m/z : 418.9 $[M+Na]^+$, 434.9 $[M+K]^+$; elemental analysis calcd (%) for $C_{25}H_{15}BF_2O_2$: C 75.79, H 3.82; found: C 76.29, H 3.93.

5a-H: Yield: 29%; 1H NMR (250 MHz, $CDCl_3$): δ = 13.64 (s, 1H), 7.95 (d, $^3J(H,H)$ = 15.3 Hz, 1H), 7.78 (d, $^4J(H,H)$ = 2.5 Hz, 1H), 7.56 (d, $^4J(H,H)$ = 2.5 Hz, 1H), 7.52 (d, $^3J(H,H)$ = 8.8 Hz, 1H), 7.34 (m, 5H), 7.14 (m, 6H), 7.02 ppm (d, $^3J(H,H)$ = 8.8 Hz, 1H); ^{13}C NMR (62.5 MHz, $CDCl_3$): δ = 191.16, 159.98, 151.24, 147.52, 146.42, 135.26, 130.58, 129.65, 127.22, 126.61, 125.91, 124.72, 123.99, 123.04, 121.34, 120.74, 115.50 ppm; MS (ESI positive mode): m/z : 460.0 $[M+H]^+$; MS (ESI negative mode): m/z : 458.1 $[M-H]^-$; elemental analysis calcd (%) for $C_{27}H_{19}Cl_2NO_2$: C 70.44, H 4.16, N 3.04; found: C 70.90, H 4.27, N 3.10.

5a: 1H NMR (250 MHz, $CDCl_3$): δ = 8.75 (d, $^3J(H,H)$ = 14.5 Hz, 1H), 8.00 (d, $^4J(H,H)$ = 2.2 Hz, 1H), 7.94 (d, $^4J(H,H)$ = 2.2 Hz, 1H), 7.89 (d, $^3J(H,H)$ = 9.0 Hz, 2H), 7.66 (m, 4H), 7.51 (m, 7H), 7.22 ppm (d, $^3J(H,H)$ = 9.0 Hz, 2H); ^{19}F NMR (235 MHz, $CDCl_3$): δ = -143.56 ($^{10}B-F$, 0.2F), -143.62 ppm ($^{11}B-F$, 0.8F); MS (ESI, positive mode): m/z : 530.1 $[M+Na]^+$, 546.1 $[M+K]^+$; elemental analysis calcd (%) for $C_{27}H_{18}BF_2Cl_2NO_2 \cdot 1/5 CH_2Cl_2$: C 62.21, H 3.53, N 2.67; found: C 62.32, H 3.71, N 2.71.

5b-H: Yield: 34%; 1H NMR (250 MHz, $CDCl_3$): δ = 14.00 (s, 1H), 8.20 (d, $^4J(H,H)$ = 1.8 Hz, 1H), 8.13 (d, $^4J(H,H)$ = 2.0 Hz, 1H), 7.94 (d, $^3J(H,H)$ = 15.0 Hz, 1H), 7.52 (d, $^3J(H,H)$ = 8.5 Hz, 2H), 7.36 (d, $^3J(H,H)$ = 14.8 Hz, 1H), 7.31 (m, 4H), 7.15 (m, 6H), 7.02 ppm (d, $^3J(H,H)$ = 8.8 Hz, 2H); ^{13}C NMR (62.5 MHz, $CDCl_3$): δ = 191.78, 161.95, 151.97, 151.21, 147.49, 146.43, 137.88, 130.56, 129.63, 126.67, 125.88, 124.68, 121.94, 120.77, 115.29, 88.46, 80.07 ppm; MS (ESI positive mode): m/z : 643.8 $[M+H]^+$; MS (ESI negative mode): m/z : 641.9 $[M-H]^-$; elemental analysis calcd (%) for $C_{27}H_{19}I_2NO_2 \cdot 1/2 CH_2Cl_2$: C 48.17, H 2.94, N 2.04; found: C 48.16, H 2.87, N 2.05.

5b: 1H NMR (250 MHz, $CDCl_3$): δ = 8.48 (d, $^3J(H,H)$ = 14.5 Hz, 1H), 8.35 (d, $^4J(H,H)$ = 2.0 Hz, 1H), 8.10 (d, $^4J(H,H)$ = 2.0 Hz, 1H), 7.63 (d, $^3J(H,H)$ = 8.8 Hz, 2H), 7.40 (m, 4H), 7.23 (m, 7H), 6.97 ppm (d, $^3J(H,H)$ = 8.8 Hz, 2H); ^{19}F NMR (235 MHz, $CDCl_3$): δ = -143.58 ($^{10}B-F$, 0.2F), -143.64 ppm ($^{11}B-F$, 0.8F); MS (ESI positive mode): m/z : 713.8 $[M+Na]^+$, 729.7 $[M+K]^+$; elemental analysis calcd (%) for $C_{27}H_{18}BF_2I_2NO_2 \cdot 1/3 (C_2H_5)_2O$: C 47.54, H 3.00, N 1.96; found: C 47.52, H 2.83, N 2.08.

Steady-state optical spectroscopy: UV/Vis-absorption spectra were measured on a Varian Cary 50. Solid-state spectra were measured by drop-casting a solution of the compound in dry CH_2Cl_2 onto a quartz plate and correcting for a scattered-light background. Emission spectra were measured on a Horiba-JobinYvon Fluorolog-3 spectrofluorimeter that was equipped with three-slit double-grating excitation and a spectrograph emission monochromator with dispersions of 2.1 nm mm^{-1} (1200 grooves mm^{-1}). Steady-state luminescence was excited by using unpolarized light from a 450 W xenon CW lamp and detected at an angle of 90° for

dilute-solution measurements (10 mm quartz cell) with a red-sensitive Hamamatsu R928 photomultiplier tube for spectra up to 700 nm and a Hamamatsu R406 photomultiplier tube for spectra above 700 nm. Special care was taken to correct NIR-emission spectra that were obtained with the latter device. According to the procedure described by Parker,^[32] we recorded the observed photomultiplier output A_i at wavelength λ , which corresponded to the apparent emission spectrum. A_i is given by [Eq. (1)], where F_i and S_i are the corrected emission spectrum and the spectroscopic sensitivity factor of the monochromator-photomultiplier setup, respectively.

$$A_i = (F_i)(S_i)/\lambda^2 \quad (1)$$

To calculate S_i , we used 4-*N,N*-dimethylamino-4'-nitrostilbene (DMANS) as a standard NIR fluorophore for which its corrected emission spectrum has been precisely determined (see the Supporting Information, Figure S14).^[33] Luminescence quantum yields (Φ_i) were measured in dilute solutions in CH_2Cl_2 with an absorbance of below 0.1 by using [Eq. (2)], where $OD(\lambda)$ is the absorbance at the excitation wavelength (λ), n the refractive index, and I the integrated luminescence intensity.

$$\Phi_{ix}/\Phi_{ir} = [OD_r(\lambda)/OD_x(\lambda)][n_x^2/n_r^2][I_x/I_r] \quad (2)$$

Subscripts "r" and "x" represent the reference compound and the sample, respectively. The luminescence quantum yields were not corrected with their refractive indices. Herein, the reference solution was ruthenium trisbipyridine bischloride in water (Φ_{ir} = 0.021) for compounds that absorbed in the 450 nm region, whilst rhodamine B (Φ_{ir} = 0.49) in EtOH was used for excitation between 540 and 560 nm. Excitation of the reference- and sample compounds was performed at the same wavelength. Solid-state luminescence quantum yields were measured on thin films for all compounds and on suspensions of colloidal aggregates in water for compounds **1b**, **2b**, and **3b**. Emission spectra were obtained by using front-face illumination. Identical values were found, within experimental error, for compounds **1b**, **2b**, and **3b** by using both techniques. The colloidal aggregate luminescence was compared to that of ruthenium trisbipyridine bischloride in water (Φ_{ir} = 0.021) and the luminescence quantum yields were calculated by using Equation (2). Molecules for which the fluorescence quantum yields of thin films could be calibrated with those obtained on aggregates were used as references for films of the other compounds. All luminescence quantum yields were measured with an absorbance below 0.1 on three different samples to minimize errors. We checked that thin films gave constant absorbance values when recorded at different places on the film surface.

Time-resolved fluorescence emission: For compounds that had very short excited-state decays (<1 ns), luminescence-lifetime measurements were performed by using time-correlated single-photon counting (TCSPC) spectroscopy. In brief, femtosecond pulses (150 fs, 800 nm, 76 MHz) that were generated by using a tunable mode-locked Ti:Sapphire laser (MaiTai HP, Spectra-Physics) were externally doubled by using a 1 mm-thick BBO crystal. The pulse-repetition rate was slowed to 7.6 MHz by using a pulse-picker (Model 3980, Spectra-Physics), thereby extending the delay between consecutive pulses to 126 ns. The generated 400 nm femtosecond pulses illuminated a 1 cm-thick cuvette that contained the solution under study. The photoexcited fluorescence was collected at a 90° geometry and sent into a subtractive double-monochromator (DH10, Jobin-Yvon) before being detected by a silicon avalanche photodiode (PDM50CTC, Micro Photon Devices). The width of the entrance- and exit slits ensured 1 nm spectroscopic resolution in the lifetime measurements. A small part of the 800 nm laser beam was selected and sent to a photodiode (TDA 200, Picoquant). The laser- and fluorescence signals were subsequently sent to a correlator (PicoHarp 300, Picoquant). Thus, the time of arrival of the fluorescence photons could be retrieved with 16 ps resolution and the fluorescence temporal decay could be reconstructed. We estimated the temporal response of the setup to be 150 ps FWHM. The instrumental response function (IRF) was systematically measured for all experimental runs. In addition, we measured the temporal response of the solvent (CH_2Cl_2) at all wavelengths. This response was then subtracted from the sample's response. Longer-lifetime meas-

measurements were carried out on a HORIBA Jobin Yvon IBH FluoroLog-3 spectrofluorimeter that was adapted for time-correlated single-photon counting. For these measurements, pulsed LEDs with an appropriate wavelength were used. Emission was monitored perpendicular to the excitation pulse and spectroscopic selection was achieved by passage through the spectrograph. A thermoelectrically cooled single-photon-detection module (HORIBA Jobin Yvon IBH, TBX-04-D) that incorporated a fast-rise-time photomultiplier tube, a wide-bandwidth preamplifier, and a picosecond-constant fraction discriminator was used as the detector. Signals were acquired by using an IBH DataStation Hub photon-counting module and data analysis was performed by using the commercially available DAS 6 decay-analysis software package from HORIBA Jobin Yvon IBH; the reported τ values are given with an estimated uncertainty of about 10%.

X-ray structure analysis: Crystals of dye **1b** that were suitable for X-ray analysis were obtained by the slow evaporation of a solution in CH₂Cl₂/cyclohexane (10:1). Powder-diffraction measurements were realized in transmission mode by using an INEL diffractometer that was equipped with a linear detector INEL CPS 120 and a quartz curved monochromator. The radiation length was 1.54056 Å, which corresponded to Cu_{Kα1}. The powder was deposited into glass capillaries with diameters of 0.5, 0.7, and 1 mm. For the samples in which the crystallites agglomerated into quite large pieces, the powder was broken into small parts with a sharp spatula; milling was not used so as to prevent any possible changes in the crystalline structure. Iodine-containing samples were deposited into capillaries with a diameter of 0.5 mm and those that contained chlorine were deposited into capillaries with a diameter of 0.7 mm to diminish the X-ray absorption into the samples and, thus, to obtain better X-ray diffraction data. The intensity data for the single-crystal X-ray-diffraction analysis of compound **1b** were collected at RT on a Bruker-Nonius KappaCCD diffractometer by using Mo_{Kα} radiation ($\lambda = 0.71073$ Å). Data collection was performed with COLLECT,^[34] cell-refinement and data-reduction were performed with DENZO/SCALEPACK.^[35] The structure was solved with SIR92^[36] and SHELXL-97^[37] was used for full-matrix least-squares refinement. Then, the H atoms were introduced at idealized positions and constrained to their parent atom during the last refinements. Graphics were generated with MERCURY 2.4.

Acknowledgements

We thank Aix Marseille Université and the CNRS for financial support. A.D. and F.F. thank Dr. O. Maury and Dr. C. Andraud for kindly providing access to their spectroscopic facilities.

- [1] a) M. Shimizu, T. Hiyama, *Chem. Asian J.* **2010**, *5*, 1516–1531; b) Y. Hong, J. W. Y. Lama, B. Z. Tang, *Chem. Commun.* **2009**, 4332–4353.
- [2] a) G. Qian, Z. Y. Wang, *Chem. Asian J.* **2010**, *5*, 1006–1029; b) V. J. Pansare, S. Hejazi, W. J. Faenza, R. K. Prud'homme, *Chem. Mater.* **2012**, *24*, 812–827.
- [3] R. Raghavachari, *Near-Infrared Applications in Biotechnology*, Marcel Dekker, New York, **2001**.
- [4] a) Y. Geerts, H. Quante, H. Platz, R. Mahrt, M. Hopmeier, A. Bohm, K. Müllen, *J. Mater. Chem.* **1998**, *8*, 2357–2369; b) T. Weil, T. Vosch, J. Hofkens, K. Peneva, K. Müllen, *Angew. Chem.* **2010**, *122*, 9252–9278; *Angew. Chem. Int. Ed.* **2010**, *49*, 9068–9093.
- [5] U. Mayerhöffer, B. Fimmel, F. Würthner, *Angew. Chem.* **2012**, *124*, 168–171; *Angew. Chem. Int. Ed.* **2012**, *51*, 164–167.
- [6] a) G. Ulrich, S. Goeb, A. De Nicola, P. Retailleau, R. Ziessel, *J. Org. Chem.* **2011**, *76*, 4489–4505; b) G. Ulrich, R. Ziessel, A. Harriman, *Angew. Chem.* **2008**, *120*, 1202–1219; *Angew. Chem. Int. Ed.* **2008**, *47*, 1184–1201; c) K. Umezawa, A. Matsui, Y. Nakamura, D. Citterio, K. Suzuki, *Chem. Eur. J.* **2009**, *15*, 1096–1106; d) M. Benstead, G. H. Mehl, R. W. Boyle, *Tetrahedron* **2011**, *67*, 3573–3601; e) Y. Kubota, J. Uehara, K. Funabiki, M. Ebihara, M. Matsui, *Tetrahedron Lett.* **2010**, *51*, 6195–6198; f) J.-H. Olivier, J. Widmaier, R. Ziessel, *Chem. Eur. J.* **2011**, *17*, 11709–11714.
- [7] a) G. Qian, B. Dai, M. Luo, D. Yu, J. Zhan, Z. Zhang, D. Ma, Z. Y. Wang, *Chem. Mater.* **2008**, *20*, 6208–6216; b) M. Shimizu, R. Kaki, Y. Takeda, T. Hiyama, N. Nagai, H. Yamagishi, H. Furutani, *Angew. Chem.* **2012**, *124*, 4171–4175; *Angew. Chem. Int. Ed.* **2012**, *51*, 4095–4099; c) X. Du, Z. Y. Wang, *Chem. Commun.* **2011**, *47*, 4276–4278.
- [8] St. v. Kostanecki, J. Tambor, *Chem. Ber.* **1899**, *32*, 1921–1926.
- [9] a) R. A. Caldwell, M. Singh, *J. Am. Chem. Soc.* **1983**, *105*, 5139–5140; b) Y. Wang, *J. Phys. Chem.* **1985**, *89*, 3799–3805; c) P. S. Patila, S. M. Dharmaparakasha, K. Ramakrishnab, H.-K. Func, R. Sai Santosh Kumard, D. Narayana Raod, *J. Cryst. Growth* **2007**, *303*, 520–524; d) C. Ruzié, M. Krayer, J. S. Lindsey, *Org. Lett.* **2009**, *11*, 1761–1764; e) L. Mager, C. Melzer, M. Barzoukas, A. Fort, S. Méry, J.-F. Nicoud, *Appl. Phys. Lett.* **1997**, *71*, 2248–2250.
- [10] T. Teshima, M. Takeishi, T. Arai, *New J. Chem.* **2009**, *33*, 1393–1401.
- [11] a) K. Rurack, M. L. Dekhtyar, J. L. Bricks, U. Resch-Genger, W. Rettig, *J. Phys. Chem. A* **1999**, *103*, 9626–9635; b) K. Rurack, J. L. Bricks, G. Reck, R. Radeaglia, U. Resch-Genger, *J. Phys. Chem. A* **2000**, *104*, 3087–3109.
- [12] a) H. Reyes, Ma. Concepcion García, B. M. Flores, H. López-Rebolledo, R. Santillán, N. Farfán, *J. Mex. Chem. Soc.* **2006**, *50*, 106–113; b) J. A. VanAllan, G. A. Reynolds, *J. Heterocycl. Chem.* **1969**, *6*, 29–35; c) A. R. Alcantara, J. M. Marinas, J. V. Sinisterra, *Tetrahedron Lett.* **1987**, *28*, 1515–1518; d) M. G. Marathey, *J. Org. Chem.* **1955**, *20*, 563–571; e) K. B. Raut, S. H. Wender, *J. Org. Chem.* **1960**, *25*, 50–52.
- [13] S. A. Agarkar, R. R. Kulkarni, V. V. Dhas, A. A. Chinchansure, P. Hazra, S. P. Joshi, S. B. Ogale, *ACS Appl. Mater. Interfaces* **2011**, *3*, 2440–2444.
- [14] a) N. N. Vasil'ev, A. Ya. Gorelenko, I. I. Kalosha, V. A. Mezhentsev, I. G. Tishchenko, V. A. Tolkachev, V. Ya. Tulach, A. P. Shkadarevich, *Zh. Prikl. Spektrosk.* **1985**, *42*, 51–55; b) T. Kotowski, A. Orzeszko, W. Skubiszak, T. Stacewicz, J. A. Soroka, *Opt. Appl.* **1984**, *14*, 267–271.
- [15] Y. Cui, Y. Zhang, P. N. Prasad, J. S. Schildkraut, D. J. Williams, *Appl. Phys. Lett.* **1992**, *61*, 2132–2134.
- [16] a) J. Massin, W. Dayoub, J.-C. Mulatier, C. Aronica, Y. Bretonnière, C. Andraud, *Chem. Mater.* **2011**, *23*, 862–873; b) U. Rösch, S. Yao, R. Wortmann, F. Würthner, *Angew. Chem.* **2006**, *118*, 7184–7188; *Angew. Chem. Int. Ed.* **2006**, *45*, 7026–7030; c) W. Z. Yuan, Y. Gong, S. Chen, X. Y. Shen, J. W. Y. Lam, P. Lu, Y. Lu, Z. Wang, R. Hu, N. Xie, H. S. Kwok, Y. Zhang, J. Zhi Sun, B. Z. Tang, *Chem. Mater.* **2012**, *24*, 1518–1528.
- [17] M. D. Gujrati, N. S. Kumar, A. S. Brown, B. Captain, J. N. Wilson, *Langmuir* **2011**, *27*, 6554–6558.
- [18] a) T. M. Figueira-Duarte, K. Müllen, *Chem. Rev.* **2011**, *111*, 7260–7314; b) F. Moggia, C. Vidolot-Ackermann, J. Ackermann, P. Raynal, H. Brisset, F. Fages, *J. Mater. Chem.* **2006**, *16*, 2380–2386.
- [19] a) M. Fourmigué, P. Batail, *Chem. Rev.* **2004**, *104*, 5379–5418; b) G. R. Desiraju, R. Parthasarathy, *J. Am. Chem. Soc.* **1989**, *111*, 8725–8726.
- [20] P.-T. Chou, M. L. Martinez, W. C. Cooper, *J. Am. Chem. Soc.* **1992**, *114*, 4943–4944.
- [21] CCDC-873726 (**1b**) contains the supplementary crystallographic data for this paper. These data can be obtained free of charge from The Cambridge Crystallographic Data Centre via www.ccdc.cam.ac.uk/data_request/cif.
- [22] F. Würthner, S. Yao, T. Debaerdemaeker, R. Wortmann, *J. Am. Chem. Soc.* **2002**, *124*, 9431–9447.
- [23] Despite the fact they do not display the typical spectroscopic characteristics of perfect H- or J-aggregates (see ref. [25]), we classified aggregates of compounds **1a** and **2a** as H- and J-like aggregates, respectively, on the basis of the spectroscopic trend of their most-intense absorption band.
- [24] J. B. Birks, *Photophysics of Aromatic Molecules*, Wiley, New York, **1970**.

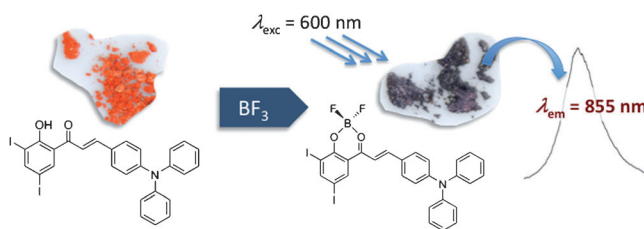
- [25] a) F. Würthner, T. E. Kaiser, C. R. Saha-Möller, *Angew. Chem.* **2011**, *123*, 3436–3473; *Angew. Chem. Int. Ed.* **2011**, *50*, 3376–3410; b) *J-Aggregates* (Ed.: T. Kobayashi), World Scientific, Singapore, **1996**.
- [26] a) J. Cornil, D. Beljonne, J.-P. Calbert, J.-L. Brédas, *Adv. Mater.* **2001**, *13*, 1053–1067; b) F. C. Spano, *Chem. Phys. Lett.* **2000**, *331*, 7–13; c) F. Meinardi, M. Cerminara, A. Sassella, A. Borghesi, P. Spearman, G. Bongiovanni, A. Mura, R. Tubino, *Phys. Rev. Lett.* **2002**, *89*, 157403.
- [27] a) J. Gao, C. Strässler, D. Tahmassebi, E. T. Kool, *J. Am. Chem. Soc.* **2002**, *124*, 11590–11591; b) H. Kashida, K. Sekiguchi, X. Liang, H. Asanuma, *J. Am. Chem. Soc.* **2010**, *132*, 6223–6230.
- [28] a) S. Jursenas, A. Gruodis, G. Kodis, M. Chachisvilis, V. Gulbinas, E. A. Silinsh, L. Valkunas, *J. Phys. Chem. B* **1998**, *102*, 1086–1094; b) V. Bulović, P. E. Burrows, S. R. Forrest, J. A. Cronin, M. E. Thompson, *Chem. Phys.* **1996**, *210*, 1–12.
- [29] H. Langhals, T. Potrawa, H. Nöth, G. Linti, *Angew. Chem.* **1989**, *101*, 497–499; *Angew. Chem. Int. Ed. Engl.* **1989**, *28*, 478–480.
- [30] a) F. C. Spano, *J. Chem. Phys.* **2003**, *118*, 981–994; b) F. Meinardi, M. Cerminara, A. Sassella, R. Bonifacio, R. Tubino, *Phys. Rev. Lett.* **2003**, *91*, 247401.
- [31] a) For a recent review, see: A. Mishra, P. Bäuerle, *Angew. Chem.* **2012**, *124*, 2060–2109; *Angew. Chem. Int. Ed.* **2012**, *51*, 2020–2067; b) H. Bürckstümmer, E. V. Tulyakova, M. Deppisch, M. R. Lenze, N. M. Kronenberg, M. Gsänger, M. Stolte, K. Meerholz, F. Würthner, *Angew. Chem.* **2011**, *123*, 11832–11836; *Angew. Chem. Int. Ed.* **2011**, *50*, 11628–11632.
- [32] C. A. Parker, *Photoluminescence of Solutions*, Elsevier, Amsterdam, **1969**.
- [33] J. R. Lakowicz, *Principles of Fluorescence Spectroscopy*, 3rd ed., Kluwer, New York, **2006**.
- [34] COLLECT, Nonius BV, Delft, The Netherlands, **2001**.
- [35] Z. Otwinowski, W. Minor, *Methods in Enzymology, in Macromolecular Crystallography, Part A, Vol. 276* (Eds.: C. W. Carter, Jr., R. M. Sweet), Academic Press, New York, **1997**, pp. 307–326.
- [36] A. Altomare, G. Casciarano, G. Giacovazzo, A. Guagliardi, M. C. Burla, G. Polidori, M. Camalli, *J. Appl. Crystallogr.* **1994**, *27*, 435.
- [37] G. M. Sheldrick, *Acta Crystallogr. A* **2008**, *64*, 112–122.

Received: May 23, 2012
Published online: ■■■■, 0000

Near-Infrared Emission

A. D'Aléo,* D. Gachet, V. Heresanu,
M. Giorgi, F. Fages* ■■■■-■■■■

Efficient NIR-Light Emission from Solid-State Complexes of Boron Difluoride with 2'-Hydroxychalcone Derivatives



Tint it black! Complexation with boron difluoride converts 2'-hydroxychalcone derivatives into strongly absorbing/emitting dyes. These darkly

colored crystalline solids exhibit NIR emission, owing to densely packed π -stacks of dipolar chromophores.